Atmospheric observations made at Oliktok Point, Alaska as part of the Profiling at Oliktok Point to Enhance YOPP Experiments (POPEYE) campaign

Gijs de Boer[1,2], Darielle Dexheimer[3], Fan Mei[4], John Hubbe[4], Casey Longbottom[3], Peter J. Carroll[4], Monty Apple[3], Lexie Goldberger[4], David Oaks[5], Justin Lapierre[5], Michael Crume[5], Nathan Bernard[5], Matthew D. Shupe[1,2], Amy Solomon[1,2], Janet Intrieri[2], Dale Lawrence[6], Abhiram Doddi[6], Donna J. Holdridge[7], Michael Hubbell[4], Mark D. Ivey[3], Beat Schmid[4]

1) Cooperative Institute for Research in Environmental Sciences, University of Colorado Boulder, Boulder, CO, 80304, USA
2) NOAA Physical Sciences Division, Boulder, CO, 80304, USA
3) Sandia National Laboratories, Albuquerque, NM, USA
4) Pacific Northwest National Laboratory, Richland, WA, USA
5) Fairweather, LLC, Anchorage, AK, USA
6) Department of Aerospace Engineering, University of Colorado Boulder, Boulder, CO, USA
7) Argonne National Laboratory, Lemont, IL, USA

Correspondence to: gijs.deboer@colorado.edu

Abstract. Between 1 July and 30 September 2018, small unmanned aircraft systems (sUAS), tethered balloon systems (TBS), and additional radiosondes were deployed at Oliktok Point, Alaska to measure the atmosphere in support of the second special observing period for the Year of Polar Prediction (YOPP). These measurements, collected as part of the "Profiling at Oliktok Point to Enhance YOPP Experiments" (POPEYE) campaign, targeted quantities related to enhancing our understanding of boundary layer structure, cloud and aerosol properties and surface-atmosphere exchange, and provide extra information for model evaluation and improvement work. Over the three-month campaign, a total of 59 DataHawk2 sUAS flights, 52 TBS flights, and 238 total radiosonde launches were completed as part of POPEYE. The data from these coordinated activities provide a comprehensive three-dimensional data set of the atmospheric state (air temperature, humidity, pressure, and wind), surface skin temperature, aerosol properties, and cloud microphysical information over Oliktok Point. These data sets have been checked for quality and submitted to the US Department of Energy (DOE) Atmospheric Radiation Measurement (ARM) program data archive (http://www.archive.arm.gov/discovery/) and are accessible at no cost by all registered users. The primary dataset DOIs are 10.5439/1418259 (DataHawk2 measurements; Atmospheric Radiation Measurement Program, 2016b), 10.5439/1426242 (TBS measurements; Atmospheric Radiation Measurement Program, 2017) and 10.5439/1021460 (radiosonde measurements; Atmospheric Radiation Measurement Program, 2013a).

1. Introduction

Recent decades have seen notable shifts in Arctic climate (Serreze et al., 2007; Screen and Simmonds, 2010). Reductions in sea ice (Maslanik et al., 2011; Comiso et al., 2008), evident as an integrator of a warming Arctic atmosphere (Dobricic et al., 2016; Graversen et al., 2008), and evolving surface energy budget (Mayer et al., 2016; Hudson et al., 2013) act to enhance absorption of solar radiation at the surface due to a dramatic shift in surface albedo (REFS), potentially enhancing Arctic warming. Sea ice reductions also present opportunities for commerce, including natural resource extraction, shipping, and fishing (Smith and Stephenson, 2013; Ho, 2010). Finally, these changes have direct implications on border security due to reduced difficulties with navigation in Arctic waters.

In recognition of the importance of these changes and our need to be able to predict and understand them, several nations have established Arctic atmospheric observatories. These observatories measure atmospheric state, cloud properties, aerosols, winds, and surface meteorology, providing critically needed datasets for assimilation into numerical weather prediction models and to advance the physical understanding of the Arctic atmosphere. In northern Alaska, the US Department of Energy (DOE) Atmospheric Radiation Measurement (ARM) Program currently operates two such observatories. The first is the long-term North Slope of Alaska (NSA) site located in Utqiagvik, which has operated since the late 1990s. Additionally, since 2013, the DOE ARM program has operated its third ARM mobile facility (AMF-3) at Oliktok Point, Alaska. Consortia such as the International Arctic Systems for Observing the Atmosphere (IASOA, Uttal et al., 2016) have formed to support the efficient synthesis of measurements from these and other observatories around the Arctic.

These observatories only represent a fraction of the work to improve our ability to predict the Arctic environment. Groups such as the World Weather Research Programme (WWRP) Polar Prediction Project (PPP) have developed concentrated efforts to support such work. An example of such an effort is the Year Of Polar Prediction (YOPP), taking place from mid-2017 through mid-2019, which directly targets the improvement of prediction capabilities across a wide variety of time scales, from hours to seasons, through coordinated and intensive observations and focused modeling activities. During the "core phase" of the YOPP, two "special observing periods" (SOPs) were conducted in 2018. This includes one SOP in spring (1 February 2018 to 31 March 2018) and one in late summer (1 July 2018 to 30 September 2018). The "core phase" will be followed by a three-year "consolidation phase", during which a variety of experiments and analysis projects will leverage the datasets collected during the core phase to evaluate and improve models, conduct data denial experiments, and evaluate the state of polar prediction.

Based on the input of the global weather and climate modeling communities, YOPP has established a set of detailed modelling priorities, including:

- *Boundary layer including mixed phase clouds*
- *S*ea ice modelling
- *Physics of coupling, including snow on sea ice*

81   •   *High resolution modelling including ensembles*
82   •   *Model validation and intercomparison*
83   •   *Upper ocean processes*
84   •   *The stratosphere*
85   •   *Chemistry, including aerosols and ozone*

86 As part of the second SOP, the DOE ARM program supported efforts to enhance observational
87 coverage of the atmosphere at the AMF-3 in Oliktok Point, Alaska (Figure 1). This project, titled
88 "Profiling at Oliktok Point to Enhance YOPP Experiments" (POPEYE) included deployment of the
89 DataHawk2 unmanned aircraft system, tethered balloon systems, and one additional radiosonde
90 per day (three launches daily versus the standard twice-daily launch schedule followed at the
91 observatory) to provide measurements needed to help meet the objectives above. The lower-
92 atmospheric thermodynamic observations offer a detailed look into the Arctic summer time
93 boundary layer providing insight into its structure and evolution, and a means of validating
94 retrieval algorithms from remote sensors. Such measurements support the stated YOPP goal of
95 pursuing an integrated modeling framework to connect cloud, boundary layer and surface energy
96 exchange schemes through Large Eddy Simulation (LES)-based development. Additionally,
97 POPEYE provides a detailed dataset that can be used for evaluation of model performance across
98 a variety of model products (e.g., reanalyses, weather forecast models, coupled regional forecast
99 models, global climate models), and more frequent radiosondes can help assess the impact of
100 data assimilation on operational models. This facilitates studies on the impact of enhanced Arctic
101 observations on predictions of lower latitude weather (e.g., Jung, 2014; Inoue et al. 2015). The
102 measurements collected can also provide constraints on the initial and boundary conditions for
103 intercomparisons of single- column and large eddy simulation models. The increased frequency
104 of radiosonde launches provides an enhanced look into the Arctic stratosphere, further
105 supported by the launch of additional radiosondes at other observatories during this SOP. Finally,
106 POPEYE aerosol measurements provide information on the vertical structure of key particle
107 properties.

108 This paper describes the dataset collected during POPEYE. Section two includes information on
109 the systems and sensors used, sampling strategies employed, limitations related to weather and
110 other factors, and a general overview of the dataset as collected. Section three provides
111 background on the data processing and quality control measures applied to the datasets
112 collected during POPEYE, and information on the different levels of data resulting from this effort.
113 Section four provides information on the availability of the data, including a link for where the
114 datasets can be downloaded. Finally, section five provides a summary of the POPEYE campaign.

115 **2. Description of Measurements and Sampling Strategy**

116 POPEYE featured a focused deployment of three observational tools during the second northern
117 hemispheric YOPP SOP. These measurements were designed to complement measurements
118 from the instruments integrated into the AMF-3, which run continuously and are therefore not
119 described in detail in this paper. The reader is referred to comprehensive information available
120 through the ARM web page (www.arm.gov). The three datasets described here are those that

121 were specifically deployed as a part of POPEYE, including the DataHawk2 small unmanned aircraft
122 system (sUAS), two tethered balloon systems (TBSs) and extra radiosondes. All systems were
123 deployed by DOE ARM operators, and the Datahawk2 and TBS systems have been deployed
124 regularly at Oliktok Point over the past few years (de Boer et al., 2018). Here we provide
125 information on these systems and the sensors operated on each.

126 **2.1. Tethered Balloon Systems**
127 TBSs mainly consisted of two different balloons, a 35 m^3 helikite constructed by Allsopp Helikites
128 and a 79 m^3 aerostat constructed by SkyDoc[TM]. The helikite is a balloon/kite hybrid that uses
129 lighter-than-air principles to obtain its initial lift, and a kite to achieve stability and dynamic lift,
130 while the larger aerostat uses a skirt instead of a kite to achieve stability in flight. Lift of both a
131 helikite and an aerostat increase with increasing wind speed, so a relatively stable float altitude
132 can be achieved even in elevated wind speeds. For POPEYE operations, both systems were
133 operated using an electric winch integrated into a dedicated balloon trailer by Sandia National
134 Laboratories. The payload and operating guidelines for the TBSs vary significantly with location
135 and environmental conditions. Generally, the aerostat is operated for total payload weights of 8
136 – 27 kg, and the helikite is operated for total payload weights < 27 kg. The helikite is not typically
137 operated above 600 m AGL, because beyond this altitude the weight of the tether and payload
138 exceed the maximum lifting force of the helikite. The aerostat can be operated at higher
139 altitudes, but due to its larger size is not launched in sustained surface wind speeds > 7 m s^{-1}. The
140 helikite is not launched in sustained surface wind speeds > 11 m s^{-1}. Operation of either platform
141 is suspended, and the balloon is immediately retrieved if sustained wind speeds at the altitude
142 of the balloon exceed 15 m s^{-1}. In general, the strength of the wind is the main limiting factor
143 governing the launch and final altitude of the TBSs, with rime accretion on the tether,
144 instruments and balloon also contributing to altitude limitations.
145
146 POPEYE TBS operations involved a variety of sensors and payloads. To measure the
147 thermodynamic properties of the atmosphere, the TBS team operated multiple different sensor
148 packages from interMet. This includes the interMet iMet-1-RSB radiosonde package as well as
149 the interMet XQ2 sensor packages developed for use on UAS. Additionally, a Silixa XT distributed
150 temperature sensing (DTS) system was flown. This system, which includes a long fiberoptic cable
151 suspended along the tether, provides a high resolution, continuous measurement of air
152 temperature based on Raman scattering (Keller et al. 2011; DeJong et al. 2015). Using this
153 system, the temperature is typically measured along the length of the optical fiber every 30 to
154 60 seconds at 0.65 cm spatial resolution. To provide information on the winds aloft, vaned cup
155 anemometers from APRS World were operated at specified intervals along the tether. It is
156 important to note that while wind speed from these sensors appears to be relatively accurate
157 when compared with Doppler lidar measurements, a variety of factors including the high latitude
158 location make the directional measurement inaccurate. Information on the aerosol particle
159 population was provided using a combination of two Handix Scientific Printed Optical Particle
160 Spectrometers (POPS) and a TSI Condensation Particle Counter (CPC) 3007. The two POPS
161 provide information on the aerosol size distribution for particles between 140-3000 nm while the
162 CPC provides information on the total number of particles between 10-1000 nm. Additionally,

163 vibrating wire sensors from Anasphere and the University of Reading provide information on the
164 amount of supercooled liquid water in cloud. These sensors were collectively referred to as
165 "Supercooled Liquid Water Content" (SLWC) sensors. Further details on all of these sensors and
166 the expected level of accuracy (where available) are included in Table 1.
167
168 The main role of the TBS in POPEYE was to collect detailed information on the vertical structure
169 of the lower atmosphere over the AMF-3. This provides information on stratification and the
170 temporal evolution of the lower atmospheric structure. Additionally, the TBS is unique in that it
171 is able to fly in and above cloud for extended time periods, providing an opportunity to collect
172 in-situ measurements of thermodynamic, aerosol and cloud microphysical properties on low-
173 altitude Arctic clouds. To accomplish this, the TBS was flown as high as weather conditions would
174 permit, conducting repeated profiles with sensors distributed along the tether. While the exact
175 placement of the sensors would change from flight to flight to adapt to the present conditions,
176 in general the system was operated with a cluster of sensors including a POPS, CPC, iMet and
177 SLWC near the top of the tether under the balloon, a DTS fiber along the entire length of the
178 tether, and subsequent iMet sensors and anemometers below the main package as most
179 desirable based on the meteorological conditions. When flying the aerostat, a second POPS
180 would also be flown to get more detailed measurements of evolution of the aerosol profile in
181 time. A schematic outlining this strategy is included in Figure 2.
182
2.2. DataHawk2 sUAS
184 Another instrument platform used during POPEYE was the Datahawk2 sUAS, developed at the
185 University of Colorado Boulder (description of the first version of the DataHawk can be found in
186 Lawrence and Balsley, 2013). The DataHawk2 sUAS is a small (1.2 m wingspan, <1 kg take- off
187 weight), robotic, pusher-prop aircraft designed to operate in a variety of conditions as a flexible
188 and inexpensive measurement platform (see Table 2 for the specifications of the DataHawk2
189 UAS). The DataHawk2 has been used for a variety of purposes, including the study of turbulence
190 (e.g. Kantha et al., 2017; Balsley et al., 2018) and high latitude (e.g. de Boer et al., 2016; 2018)
191 deployments. The relatively slow flight speed (14 m/s, burst up to 22 m/s) allows the platform
192 to obtain measurements at high spatial resolution when compared to other aerial vehicles.
193 Despite this relatively slow speed, the DataHawk2 has been operated in winds up to 12 m/s,
194 making it a robust research platform for the harsh Arctic environment. DataHawk2 flights
195 completed under POPEYE were generally autopilot guided except for during take-off and landing,
196 when they were under the control of a local pilot through real-time telemetry. All flights were
197 completed within radio communication range and within sight of the ground operators and were
198 conducted within restricted airspace (R-2204, see Figure 1, de Boer et al., 2016) controlled by the
199 US DOE. This allowed operators to adjust the flight plan in real time to meet the needs of the
200 science objectives and adapt to the changing environment. The ground controller and UAS
201 communicate via 2.4 GHz radio with a range of approximately 10 km. Regulations limit
202 DataHawk2 flight to within visual line of sight, meaning that it is not allowed to fly into clouds
203 and follow VFR weather minimums for operation (14 CFR 91.155). Additionally, winds hamper
204 the operation of the DataHawk2, with DOE ARM guidelines restricting flight when winds top 7 m
205 s^{-1}.

206 The DataHawk2 carries a variety of sensors to make measurements of the atmospheric and
207 surface states. Custom-built instrumentation includes a fine wire sensor employing two cold- and
208 one hot-wire. These provide high-frequency (800 Hz) information on temperature and fine scale
209 turbulence. High bandwidth is enabled by small surface-area-to-volume ratios of very thin (5 µm
210 diameter) wires. In addition, the DataHawk2 carries a custom configuration that includes
211 integrated-circuit slow response sensors (Sensiron SHT-31) for measurement of temperature
212 through a calibrated semiconductor, and relative humidity using a capacitive sensor. For POPEYE
213 specifically, the DataHawk2 also carried an E+E EE03 digital temperature and humidity
214 (capacitive) sensor that was externally mounted on the airframe. For information on surface and
215 sky temperatures, DataHawk2s are equipped with up- and downward-looking thermopile sensors
216 (Semitec 10TP583T with custom electronics). These sensors undergo a calibration using targets
217 of a known temperature. Finally, DataHawk2s have also carried the commercially-available iMet1
218 radiosonde package, providing comparative information on position (GPS), temperature (bead
219 thermistor), pressure (piezoresistive) and relative humidity (capacitive), though these sensors
220 were not installed during POPEYE.
221 The main objective for the DataHawk2 was to obtain as many profiles as possible of the lower
222 atmosphere during daytime hours. To do this, the aircraft was programed to climb from the
223 surface to the maximum obtainable altitude. This maximum altitude was constrained by the
224 pilot's ability to maintain visual contact with the aircraft (1000 m AGL) or by the cloud ceiling.
225 Because the endurance of the aircraft is approximately 50 minutes in Arctic operating conditions,
226 the aircraft could generally complete between one and two full profiles before needing to land
227 to change batteries. The turnaround time between flights can be as short as 10 minutes, but is
228 generally on the order of 15-30 minutes. Because of the substantial interest in the interplay
229 between thermodynamic and dynamic properties near cloud base, during cloudy conditions, the
230 operators were requested to hold altitude around the cloud base height, as determined from the
231 observatory ceilometer and visual tracking of the aircraft, for 10-15 minutes to collect statistics
232 of that environment before descending back towards the surface. While the cloud base height
233 is variable, ideally the altitude held by the aircraft would be within 25 m of the mean cloudbase
234 level. Figure 3 provides an illustration outlining this flight pattern.
235
236   **2.3. Radiosondes**
237 The DOE ARM program launched Vaisala RS-92 radiosondes on a regular schedule under POPEYE.
238 Due to concerns about operator safety and fatigue, the number of radiosondes launched was
239 scheduled at three per day, with requested launch times of 05:30, 17:30 and 23:30 UTC (21:30,
240 09:30, 15:30 AKDT) to match the 06:00, 18:00 and 00:00 UTC synoptic times. Radiosonde
241 launches were at times suspended due to dangerous conditions, including the presence of bears
242 on site, or high winds (>13.5 m s^{-1} sustained and gusting >18 m s^{-1}) which could result in damage
243 to the sensor package if the balloon does not achieve enough vertical lift due to the strong cross
244 wind. Radiosondes are lifted using 350g balloons with an average ascent rate target of 5.5 ms^{-1}.
245 Radiosonde data from the campaign are available through the ARM data archive (Atmospheric
246 Radiation Measurement program, 2013a).
247
248   **2.4. Overview of meteorological conditions sampled**

249   The presence of the ARM AMF-3, allows us to put the measurements from the radiosondes, TBS
250   and UAS in broader context. Figure 4 shows measurements from the AMF-3 surface
251   meteorological instrumentation (Atmospheric Radiation Measurement Program, 2013b) over the
252   three-month POPEYE period. Synoptically, this period featured several driving features. For
253   much of the campaign, there was a stationary area of high pressure positioned over the Gulf of
254   Alaska, and Oliktok Point sat on the gradient between this area of high pressure and transient
255   low pressure systems moving through the Chukchi and Beaufort Seas. This generally resulted in
256   west-northwesterly winds during this time period. Some of these cyclones passed closer to
257   shore, thereby directly impacting the Oliktok Point area and creating precipitation events and
258   shifting wind regimes (e.g. July 7-10; August 13; August 16-17; August 29-31). In late August
259   there was a general shift in the pattern with high pressure beginning to set up over northern
260   Alaska and eventually over the Beaufort Sea to the north. This resulted in a general shift towards
261   easterly winds at the surface. The end of the POPEYE campaign featured a dominant area of high
262   pressure over the area, resulting in weak easterly winds.
263
264   Considering the vertical structure of the lower atmosphere, the observations included
265   measurements from a variety of stability regimes. While the presence of the sun in summer
266   months generally results in more adiabatic lower atmospheric states than during other times of
267   year in the Arctic, the data collected indicates sampling of both well-mixed and stratified
268   conditions. This includes several stable boundary layer cases. Additionally, many of the
269   completed flights were flown with some level of cloud cover in place. While the UAS did not
270   sample through the cloud, the TBS was able to do so, providing insight into the thermodynamic
271   and microphysical structure in and around these clouds. Based on ceilometer data from the AMF-
272   3 (Atmospheric Radiation Measurement Program 2013c), a cloud base was detected during 76%
273   of the campaign period. Of the times when clouds were detected, 73% of the cloud bases
274   occurred below 1 km altitude, 21% occurred between 1-4 km altitude, and 6% were found above
275   4 km.
276
277   In general, it is relevant and important to note that to some extent all of the POPEYE platforms
278   were weather-limited in terms of their operations. Therefore, there is an element of selective
279   sampling to consider when using the collected datasets. Most directly, the TBS and UAS systems
280   were generally not operated during high winds. The UAS additionally had limitations related to
281   visibility.   The radiosondes were least impacted, though high winds did also prevent some
282   launches.
283

284   **2.5. Overview of completed flights and radiosonde launches**
285   Over the three-month period, there were limited data outages and challenges related to the
286   issues discussed in the previous sections. Figure 5 illustrates the operations completed under
287   POPEYE. The most significant challenge to continuous operations was the electromagnetic
288   interference (EMI) caused by a US Air Force radar station at Oliktok Point, located approximately
289   150-300 m from the DataHawk2 flight areas. Modifications made to this radar during the POPEYE
290   time window unfortunately resulted in the grounding of the DataHawk2s for their planned
291   second and third deployments. Additionally, this EMI resulted in some resets of the TBS
292   instrumentation, and errors in the TBS GPS readings.   In addition, there were some challenges

293   associated with the Arctic weather. Despite it being summer, winds were a challenge to both
294   TBS and UAS flights at times, and also resulted in the cancellation of some radiosonde launches.
295   Wildlife also posed challenges, as the site is visited by both brown and polar bears during the
296   summer months. The local presence of these large creatures generally required that operators
297   ceased outdoor operations, impacting all three measurement platforms.   Despite these
298   challenges, the campaign totaled 238 radiosondes launched, 52 TBS flights (134.3 flight hours),
299   and 59 DataHawk2 flights (64.6 flight hours). Figure 6 illustrates the completed flights in time-
300   height space.
301
302   A map indicating the horizontal extent of the TBS flights is shown in Figure 7 (top). The horizontal
303   distances covered are governed by the positioning of the winch trailer for the system, the wind
304   speed, and the amount of tether extended. The points drifting over the ocean surface are the
305   result of erroneous GPS data, likely linked to EMI from the USAF radar system. The distribution
306   balloon altitudes (the highest sampling height for any given TBS operation) is shown in Figure 7
307   (bottom) and demonstrates that the balloon typically sampled the lowest 1 km of the
308   atmosphere. Because the balloon can hover at a given altitude for extended time periods, there
309   are multiple peaks in the altitude distribution, notably at around 150 m, 300 m, 700 m and 1000
310   m. These altitudes correspond to altitudes chosen for extended sampling during the campaign.
311   Also, a comparison of TBS altitudes with ceilometer-based cloud base measurements indicates
312   that the TBS was operating at or above the lowest detected cloud base altitude 32% of the time.
313
314   A map of the horizontal extent of the DataHawk2 flights is shown in Figure 8 (top). All flights
315   were conducted in close proximity to the AMF-3 instrumentation, within the restricted airspace
316   outlined under R-2204. The flight patterns consisted of profiling of the lowest 1 km of the
317   atmosphere, as indicated by the probability distribution of altitudes sampled in the lower panel.
318   This distribution is binned by 20 m increments and based on this it becomes clear that most
319   common altitude was between 20-40 m above ground level (AGL). From this altitude, the
320   frequency of visiting higher altitudes generally decreases slowly, resulting from limitations
321   imparted by visibility and winds.
322
323   Figure 9 provides insight into the statistics of the radiosonde measurements. The right panel
324   indicates the distance away from Oliktok Point that radiosondes traveled over the length of the
325   POPEYE campaign. Within the troposphere (<10 km altitude), radiosondes generally remained
326   within 20 km of the Oliktok Point facility. However, a few balloons traveled as far as 100 km away
327   once in the stratosphere, with most staying within 50 km of the site all the way to the top of the
328   profile. The temperature-height histogram (figure 6, left panel) reveals a general cooling of the
329   air with height through the depth of the troposphere, with most profiles cooling from
330   temperatures of 0-10 C near the surface to around -50 C at the tropopause. Additionally, there
331   are indicators of frequent low-level inversions in the lowest 1-2 km. There appear to be two
332   modes of temperatures observed in the stratosphere, with a dominant mode between -40 and -
333   50 C, and a secondary mode at around -55 C. Finally, a two-dimensional histogram of the winds
334   with height (Figure 6, middle panel) illustrates a broad range of measurements near the surface
335   (0-20 m s^{-1}), with winds generally increasing with height through the troposphere to values
336   ranging between 5-50 m s^{-1}. Winds in the stratosphere again decrease to less than 10 m s^{-1}.

337 Figure 10 illustrates time-height cross sections of radiosonde measurements of temperature,
338 relative humidity and wind speed for the duration of POPEYE.
339 Finally, Figure 11 provides an initial glimpse into measurements from the POPS sensor on the
340 TBS. The top panel illustrates the cumulative number concentrations sampled, showing that the
341 range of particle numbers measured tended to decrease with height, and that higher
342 concentrations were typically sampled in the lowest parts of the atmosphere. This is likely a
343 result of the numerous near-surface sources associated with oil production facilities in the vicinity
344 of Oliktok Point. Additionally, there is some level of contamination very close to the surface from
345 the diesel generator used to run the TBS winch system. The extent of this contamination is a
346 function of wind speed and atmospheric mixing state and cannot be generally quantified. The
347 second panel shows a similar two-dimensional histogram for particle sizes. This figure illustrates
348 that most particles sampled were around 200 nm and that the balloon typically operated below
349 500 m. Again. The spread of diameters measured appears to increase with decreasing height.
350 For both of the top panels it is important to keep in mind that white areas do not necessarily
351 mean that zero samples were observed in that bin, as the lowest colorbar bin has some finite
352 edges. The bottom panel shows the relationship between particle size and concentration as a
353 function of altitude as observed over the campaign. There are numerous near-surface (dark blue)
354 points where high concentrations of smaller particles were observed. These observations are
355 complimented by measurements from the CPC for the majority of campaign flights (not shown).
356
357 **3. Data processing and quality control**
358 The US DOE ARM program handles all data collection, quality control, and processing for field
359 campaigns. In general, several different levels of ARM data are made available, ranging from raw
360 data as recorded by the sensors (a-level), to quality-controlled data (b-level) and data products
361 (c-level). This section provides an overview of the processing and quality control applied to the
362 data streams coming from the platforms deployed during POPEYE.
363
364 For the DataHawk, current processing techniques provide both raw and processed datafiles.
365 Aircraft performance and sensor data are gathered and stored in a binary format on the onboard
366 SD card. This binary format data is the raw data that is archived by ARM (a0 level). Typically, this
367 raw data is invisible to the community user, but can be requested through the ARM data
368 discovery tool if desired. In addition, the data on the SD card is unpacked, downsampled to 10
369 Hz, and assigned to a relevant array of variable names, and then exported to NetCDF format as a
370 processed raw data file (a1 level). This data file includes data gathered by onboard sensors during
371 flight, aircraft performance data, telemetry data and GPS data. The next file that is produced is a
372 10 Hz quality-controlled file that includes some initial conversions (b1 level). For example, raw
373 sensor data from the cold wire sensor and onboard temperature sensors are used to convert the
374 voltage reported by the cold wire into a temperature value. Additionally, relative humidity and
375 infrared temperature values measured are calibrated and converted from the engineering to
376 relevant physical units. Wind components are reconstructed using corrected pitot airspeed data,
377 GPS data, and the aircraft principle axis data to produce wind speed and direction and the three
378 wind components. Finally, a quality control step is applied to remove any significant spikes in the
379 dataset. This quality-controlled dataset is the current final ARM data product for DataHawk2. An

380 additional higher frequency data product is under development for future release, which will
381 provide the turbulence parameters as a value added product (VAP).
382
383 Most of the TBS measurements undergo a similar processing and quality control procedure.   In
384 particular, several quality control measures are implemented on the POPS instrument. Included
385 in this processing is a size correction that is determined through routine size checks and
386 calibration. For the size check, 500 nm polystyrene latex (PSL) particles are generated to evaluate
387 the signal response from the POPS instrument and confirm that the instrument performance is
388 steady over the course of the campaign. For the calibration, eight different PSL particle sizes are
389 used to determine the relationship between the optical response signal and particle size. In
390 addition, a flow correction is applied, which is based on routine checks using a flow meter. For
391 the CPC, routine calibrations are conducted to ensure that the flow rate is correct. Additionally,
392 ground-based comparisons are conducted with other butanol CPCs to ensure that measured
393 particle concentrations are within 15% of one another. Also, daily zero count checks are
394 completed, and the alcohol wick is recharged and replaced as needed while the instrument is
395 deployed to the field. Finally, CPC data are flagged as "questionable" when particle
396 concentrations are higher than 10^5 cm^{-3}, because of a lack of correction for coincident sampling
397 at high concentrations.
398
399 Radiosonde data are processed as quality-controlled measurements, with quality control being
400 completed proprietary Vaisala software that corrects for sensor response time and solar
401 radiation exposure.
402
403 **4. Data Availability**
404 The data files from POPEYE observations are available for public download through the US DOE
405 ARM Program Data Archive (http://www.archive.arm.gov/discovery/). ARM uses NetCDF as the
406 standard data file format, with self-describing metadata provided to the user inside the NetCDF
407 file. The data are posted as individual datastreams on the archive, which is searchable by site (in
408 this case OLI for Oliktok Point) and instrument (in this case "TBS" for the tethered balloons,
409 "aafdatahawk" for the DataHawk2, and "sonde" for the radiosondes). Each instrument may have
410 several different levels of data available.
411 The main TBS datastream for measurements from the iMet instruments and basic information
412 on aerosol instrumentation is *olitbsimetM1.a1* (DOI: 10.5439/1246367). ARM is currently
413 working to produce a quality-controlled b1 product. Data from the DTS system has been
414 collected by the ARM Data Management Facility (DMF), and can be requested by email to
415 armarchive@ornl.gov, with the appropriate DTS datastreams for POPEYE being *tbsdtssxforjch1*,
416 *tbsdtssxforjch2*, *tbsdtssxch1*, *tbsdtssxch2*. SLW sensor data is available through the ARM archive
417 under the *tbsslwc.b0* datastream, while the TBS aerosol instrumentation can also be downloaded
418 through the archive as *tbscpcM1.00*, *tbspopdryM1.00*, *tbspopwetM1.00*. All of these datasets
419 are currently provided at 1 Hz. TBS ground station data, including temperature, humidity,
420 pressure and winds at the surface, are available as b-level files on the archive under the file prefix
421 "olitbsgroundM1" as 10-minute average values.
422

423 Quality-controlled DataHawk data can be downloaded as *oliaafdatahawkmetU1.b1* (DOI:
424 10.5439/1426242). Finally, the POPEYE radisonde dataset is available as a QC'd b1 dataset, with
425 the filenames being of the general form olisondewnpnM1.b1 (DOI: 10.5439/1021460), where
426 wnpn" refers to the mode of the sonde data collection. Here, "w"=winds, "p"=PTU (pressure,
427 temperature, humidity), and "n"=nominal indicates a normal flight with data collection during
428 ascent only.
429
430 To make it possible for scientists to cite DOE ARM program data in their publications, ARM
431 recognizes the value of Digital Object Identifiers (DOIs). Such DOIs are generally being generated
432 at the ARM data product level. Data products produced from the a-level data may have their
433 own DOI -- for example, separate DOIs are assigned to each of the available output datastreams
434 and any value-added products (VAP) from the radiosonde measurements obtained by ARM. This
435 means that it is possible that POPEYE measurements could be spread across a variety of DOIs,
436 and that additional DOIs could be created that include POPEYE data as additional data products
437 are developed.

438 **5. Summary**

439 Between 1 July and 30 September 2018, the POPEYE measurement team collected detailed
440 measurements of the lower Arctic atmosphere at Oliktok Point, Alaska using tethered balloons,
441 unmanned aircraft and radiosondes. This activity resulted in the completion of 134.3 TBS flight
442 hours, 64.6 sUAS flight hours, and 238 radiosonde launches. The primary focus of POPEYE was
443 to provide detailed measurements of the lower atmosphere, including thermodynamic state,
444 aerosol properties, cloud microphysical properties, winds, and surface temperature. UAS flights
445 covered the atmosphere between the surface and 1 km altitude but were unfortunately called-
446 off early due to EMI from the nearby long-range surveillance radar system operated by the US
447 Air Force. Tethered balloon measurements went as high as 1396 m using two different balloons.
448 Radiosondes were launched at a frequency of three times daily, except when environmental
449 conditions (winds > 13.1 m s^{-1}, bears) prevented balloon launches. These datasets provide a
450 detailed look into processes in the lower atmosphere and set the stage for detailed evaluation of
451 numerical models and, together with ongoing, continuous measurements from the AMF-3,
452 support the development of modeling case studies for process understanding and evaluation of
453 parameterization performance.

454 Quality-controlled versions of the data collected as a part of POPEYE are available on the US DOE
455 ARM data archive. This archive is publicly accessible and allows users to download data from
456 these platforms and all other ARM-operated instrumentation, including measurements from the
457 AMF-3 deployment at Oliktok Point.

458
459 **Author Contributions**
460 GdB designed the field campaign, acted as principal investigator for POPEYE, conducted field
461 work as part of POPEYE, and led the development of the manuscript. DD, CL and MA were the
462 primary TBS operators during POPEYE, contributed to the processing of TBS data, and contributed

to the writing and review of the manuscript. JH, PC, and LG were the primary DataHawk2 operators during POPEYE and contributed to the processing of DataHawk2 data and the writing and review of the manuscript. DO, JL, MC and NB are site operators at Oliktok Point and conducted the radiosonde launches, contributed to site operations during POPEYE and assisted the DataHawk2 and TBS teams while in the field. FM is the instrument mentor for TBS aerosol instrumentation as well as for the DataHawk2 and contributed to data preparation and processing for POPEYE as well as manuscript writing and review. MS, AS, and JI are POPEYE Co-PIs and contributed to campaign planning, field work, and oversight as well as the writing and review of this manuscript. DL is the primary DataHawk2 developer and contributed to the development and review of the DataHawk2 dataset. AD helped with the development of wind estimation techniques using the DataHawk2. DH is the ARM instrument mentor for the radiosondes and contributed to the processing of the radiosonde dataset as well as the writing and review of this manuscript. Finally, MI and BS manage the teams responsible for operation of the TBS and DataHawk2. Additionally, MI is the primary site manager at the AMF-3. They both oversaw and supported campaign activities and additionally contributed to the review of this manuscript.

Acknowledgments

This work was supported by the US Department of Energy Atmospheric Radiation Measurement Program. Support for campaign planning and execution was provided by the US DOE Atmospheric System Research Program under project DE-SC0013306. Finally, additional support was provided by the NOAA Physical Sciences Division. We would like to thank the US Air Force for providing access to the Oliktok Point facility, ENI Petroleum who supported our teams at their Nikaitchuq Operations Center, and ConocoPhillips who housed team members at the Kuparuk camp. Finally, POPEYE is an officially-endorsed contribution to the Year of Polar Prediction (YOPP), a flagship activity of the Polar Prediction Project (PPP), initiated by the World Weather Research Programme (WWRP) of the World Meteorological Organisation (WMO). We acknowledge the WMO WWRP for its role in coordinating this international research activity.

References

Atmospheric Radiation Measurement (ARM) user facility. Updated hourly. Balloon-Borne Sounding System (SONDEWNPN). **2018-07-01** to **2018-10-01**, **ARM Mobile Facility (OLI) Oliktok Point, Alaska; AMF3 (M1)**. Compiled by D. Holdridge, J. Kyrouac and R. Coulter. ARM Data Center. Data set accessed **2018-11-08** at http://dx.doi.org/10.5439/1021460, 2013a.

Atmospheric Radiation Measurement (ARM) user facility. Updated hourly. Surface Meteorological Instrumentation (MET). **2018-07-01** to **2018-10-01**, **ARM Mobile Facility (OLI) Oliktok Point, Alaska; AMF3 (M1)**. Compiled by D. Holdridge and J. Kyrouac. ARM Data Center. Data set accessed **2018-11-08** at http://dx.doi.org/10.5439/1025220, 2013b

Atmospheric Radiation Measurement (ARM) user facility. Updated hourly. Ceilometer (CEIL). **2018-07-01** to **2018-10-01**, **ARM Mobile Facility (OLI) Oliktok Point, Alaska; AMF3**

(M1). Compiled by B. Ermold and V. Morris. ARM Data Center. Data set accessed **2018-11-08** at http://dx.doi.org/ 10.5439/1181954, 2013c.

Atmospheric Radiation Measurement (ARM) user facility. Updated hourly. Tethered Balloon System (TBSGROUND). **2018-07-01** to **2018-10-01**, **ARM Mobile Facility (OLI) Oliktok Point, Alaska; AMF3 (M1)**. Compiled by D. Dexheimer and Y. Shi. ARM Data Center. Data set accessed **2018-11-16** at http://dx.doi.org/10.5439/1246367, 2016a.

Atmospheric Radiation Measurement (ARM) user facility. Updated hourly. Tethered Balloon System (TBSIMET). 2017-04-09 to 2018-09-28, ARM Mobile Facility (OLI) Oliktok Point, Alaska; AMF3 (M1). Compiled by D. Dexheimer and Y. Shi. ARM Data Center. Data set accessed 2019-03-11 at http://dx.doi.org/10.5439/1426242, 2017.

Atmospheric Radiation Measurement (ARM) user facility. Updated hourly. Meteorological Instrumentation aboard Aircraft (AAFDATAHAWKMET). 2016-06-06 to 2018-08-07, ARM Mobile Facility (OLI) DataHawk Unmanned Aerial System (U1). Compiled by F. Mei and J. Hubbe. ARM Data Center. Data set accessed 2019-03-11 at http://dx.doi.org/10.5439/1418259, 2016b.

Balsley, B.B., Lawrence, D.A., Fritts, D.C., Wang, L., Wan, K., and Werne, J.: Fine Structure, Instabilities, and Turbulence in the Lower Atmosphere: High-Resolution In Situ Slant-Path Measurements with the DataHawk UAV and Comparisons with Numerical Modeling. *J. Atmos. Oceanic Technol.,* **35**, 619–642,https://doi.org/10.1175/JTECH-D-16-0037.1, 2018.

Comiso, J.C., Parkinson, C.L. , Gersten, R. and Stock, L.: Accelerated decline in the Arctic sea ice cover, *Geophys. Res. Lett.*, **35**, L01703, 2008.

de Boer, G., Ivey, M.D., Schmid, B., Lawrence, D., Dexheimer, D., Mei, F., Hubbe, J., Hardesty, J.O.E., Bendure, A., Shupe, M.D., McComiskey, A., Telg, H., Schmitt, C., Matrosov, S., Brooks, I., Creamean, J.M., Solomon, A., Turner, D.D., Williams, C., Maahn, M., Argrow, B., Palo, S., Long, C.N., Gao, R.-S. and Mather, J.: A Bird's Eye View: Development of an Operational ARM Unmanned Aerial Systems Capability for Atmospheric Research in Arctic Alaska, *Bull. Amer. Meteor. Soc.*, **99**, 1197-1212, https://doi.org/10.1175/BAMS-D-17-0156.1, 2018.

de Boer, G., Ivey, M.D., Schmid, B., McFarlane, S. and Petty, R.: Unmanned platforms monitor the Arctic atmosphere, *EOS*, **97**, doi:10.1029/2016EO046441, 2016.

Dobricic, S., Vignati, E. and Russo, S.: Large-scale atmospheric warming in winter and the Arctic sea ice retreat, *J. Clim.,* **29**, 2869-2888, 2016.

Graversen, R.G., Mauritsen, T., Tjernström, M., Källén, E. and Svensson, G.: Vertical structure of recent Arctic warming, *Nature*, **451**, 53-56, 2008.

Ho, J.: The implications of Arctic sea ice decline on shipping, Marine Pol., **34**, 713-715, 2010.

Hudson, S.R., Granskog, M.A., Sundfjord, A., Randelhoff, A., Renner, A.H.H. and Divine, D.V.: Energy budget of first-year Arctic sea ice in advanced stages of melt, *Geophys. Res. Lett.*, **40**, 2679-2683, 2013.

Inoue, J., Yamazaki, A., Ono, J., Dethloff, K., Maturilli, M., Neuber, R., Edwards, P. and Yamaguchi, H.: Additional Arctic observations improve weather and sea-ice forecasts for the Northern Sea Route, *Sci. Report.*, **5**, 16868, 2015.

Jung, T., Kasper, M.A., Semmler, T. and Serrar, S.: Arctic influence on sub-seasonal midlatitude prediction, *Geophys. Res. Lett.*, **41**, 3676-3680, 2014.

546 Kantha, L., Lawrence, D., Luce, H., Hashiguchi, H., Tsuda, T., Wilson, R., Mixa, T. and Yabuki, M.:
547   Shigaraki UAV-Radar Experiment (ShUREX): overview of the campaign with some preliminary
548   results, *Prog. Earth. Planet. Sci.*, **4**, 19, 2017.

549 Lawrence, D.A. and Balsley, B.B.: High-Resolution Atmospheric Sensing of Multiple Atmospheric
550   Variables Using the DataHawk Small Airborne Measurement System. *J. Atmos. Oceanic*
551   *Technol.,* **30**, 2352–2366, https://doi.org/10.1175/JTECH-D-12-00089.1, 2013.

552 Maslanik, J., Stroeve, J., Fowler, C. and Emery, W.: Distribution and trends in Arctic sea ice age
553   through spring 2011, *Geophys. Res. Lett.*, **38**, L13502, 2011.

554 Mayer, M., Haimberger, L., Pietschnig, M. and Storto, A.: Facets of Arctic energy accumulation
555   based on observations and reanalyses 2000-2015, *Geophys. Res. Lett.*, **43**, 10420-10429,
556   2016.

557 Screen, J.A. and Simmonds, I.: The central role of diminishing sea ice in recent Arctic temperature
558   amplification, *Nature*, **464**, 1334-1337, 2010.

559 Serreze, M.C., Holland, M.M. and Stroeve, J.: Perspectives on the Arctic's shrinking sea ice cover,
560   *Science*, **315**, 1533-1536, 2007.

561 Smith, L.C. and Stephenson, S.R.: New Trans-Arctic shipping routes navigable by midcentury,
562   *PNAS*, **110**, E1191–E1195, 2013.

563 Uttal, T., Starkweather, S., Drummond, J.R., Vihma, T., Makshtas, A.P., Darby, L.S., Burkhart, J.F.,
564   Cox, C.J., Schmeisser, L.N., Haiden, T., Maturilli, M., Shupe, M.D., de Boer, G., Saha, A.,
565   Grachev, A.A., Crepinsek, S.M., Bruhwiler, L., Goodison, B., McArthur, B., Walden, V.P.,
566   Dlugokencky, E.J., Persson, P.O.G., Lesins, G., Laurila, T., Ogren, J.A., Stone, R., Long, C.N.,
567   Sharma, S., Massling, A., Turner, D.D., Stanitski, D.M., Asmi, E., Aurela, M., Skov, H.,
568   Eleftheriadis, K., Virkkula, A., Platt, A., Førland, E.J., Iijima, Y., Nielsen, I.E., Bergin, M.H.,
569   Candlish, L., Zimov, N.S., Zimov, S.A., O'Neill, N.T., Fogal, P.F., Kivi, R., Konopleva-Akish, E.A.,
570   Verlinde, J., Kustov, V.Y., Vasel, B., Ivakhov, V.M., Viisanen, Y., and Intrieri, J.M.: International
571   Arctic Systems for Observing the Atmosphere: An International Polar Year Legacy
572   Consortium. *Bull. Amer. Meteor. Soc.,* **97**, 1033–1056,https://doi.org/10.1175/BAMS-D-14-
573   00145.1, 2016.

574
575

576 **Tables**

577

578 **Table 1:** Known performance characteristics for TBS instruments. The asterisk with wind
579 direction denotes that these stated specifications have not been met in the Arctic environment
580 at Oliktok Point.

581

582

	Resolution	Accuracy	Range	Response Time
iMet-1-RSB				
Pressure [hPa]	< 0.01	+/- 0.5	2 - 1070	< 1 s
T [°C]	< 0.01	+/- 0.2	-95 to 50	2 s
RH [%]	< 0.1	+/- 5	0 - 100	2 s @ 25 °C
GPS Altitude [m, MSL]		+/- 15	0 – 30+ km	
GPS Position [deg]		+/- 10		
iMet XQ2				
Pressure [hPa]	0.01	+/- 1.5	10 - 1200	10 ms
T [°C]	0.01	+/- 0.3	-90 to 50	1 s @ 5 m/s flow
RH [%]	0.1	+/- 5	0 - 100	5.2 s @ 5 °C
APRS World Wind Vane				
Wind Speed [m s^{-1}]	0.1	+/- 0.1 or 5% (whichever is greater)	1 - 59	
Wind Direction* [deg]	1	+/- 2	0 – 360	
POPS				
Particles Conc. [cm^{-3}]		+/- 10 % < 1000 cm^{-3} at 0.1 LPM	0-1250 cm^{-3}	
CPC				
Particles Conc. [cm^{-3}]		+/- 2.5-3%	0-1E^4 cm^{-3}	
TBS Ground Station				
T [°C]	0.01	+/- 0.3	-95 to 50	< 1 s
RH [%]	0.1	+/- 2 @ 20 °C, < 90% RH, +/- 3 @ 20 °C, >= 90% RH+/- 0.3	0.8 - 100-95 to 50	15 s @ 20 °C < 1 s

583

584   **Table 2:** Known performance characteristics for DataHawk2 instruments. Note that accuracy
585   estimates on wind values are estimated based on recent intercomparison with surface-based
586   instrumentation, and apply to a higher-order derived product.
587

Data Type	Resolution	Accuracy	Range	Response Time
GPS position [deg]	0.010	+/- 10 m	-180 to 180 (lon), -90 to 90 (lat)	1s
GPS altitude [m, MSL]	0.010	+/- 10 m	-100 to 15000	1s
Baro pressure [mbar]	0.01	+/- 2.5	500 to 1030	0.022 s
Rel. humidity [%]	0.01	+/- 3	0 to 105	8 s
Slow temp. [°C]	0.015	+/- 2	-40 to 80	2 s
Coldwire Voltage [V]	0.0000078 [~0.025°C]	Unknown	-40 to +80 °C	0.5 ms @ 15 m/s
Airspeed [m/s]	0.01	0.2	0 to 30	0.3 ms
iMet, EE03, Temp [°C]	0.01	+/- 0.3 deg	-40 to + 85 deg C	1s
iMet, EE03, RH [%]	0.01	+/- 3%	0-95%	1s
wind_speed [m/s]	0.01	+/- 1 m/s	0 to 100	0.1s
wind_direction [deg]	0.01	+/- 15 deg	0 to 360	0.1s
Vertical velocity (m/s)	0.01	+/- 0.2 m/s	**-100 to 100**	0.1s

588
589

590 **Figures**
591
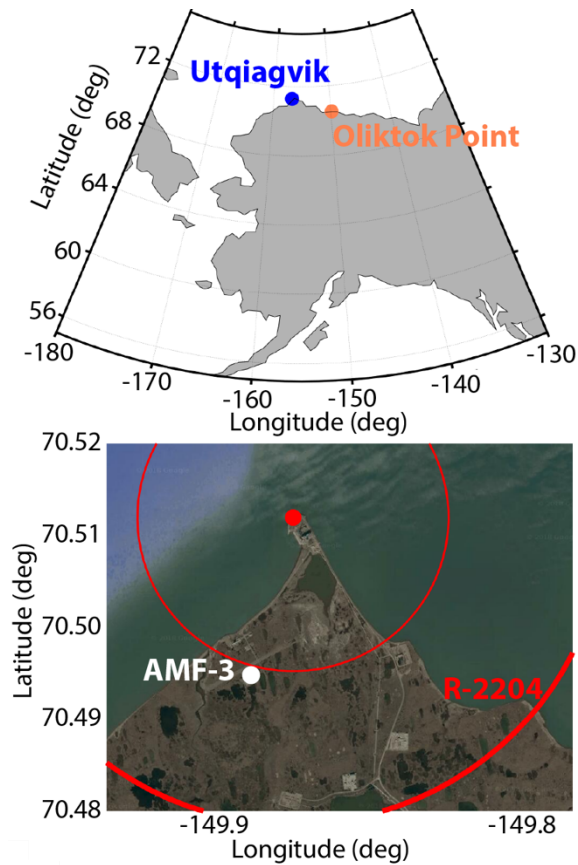
592
593 **Figure 1:** A map illustrating the location of Oliktok Point, Alaska (top). The lower panel is a
594 satellite image of the Oliktok Point area, including information on the boundaries of the R-2204
595 restricted airspace (bold red line), and the location of the DOE AMF-3 (white dot).
596
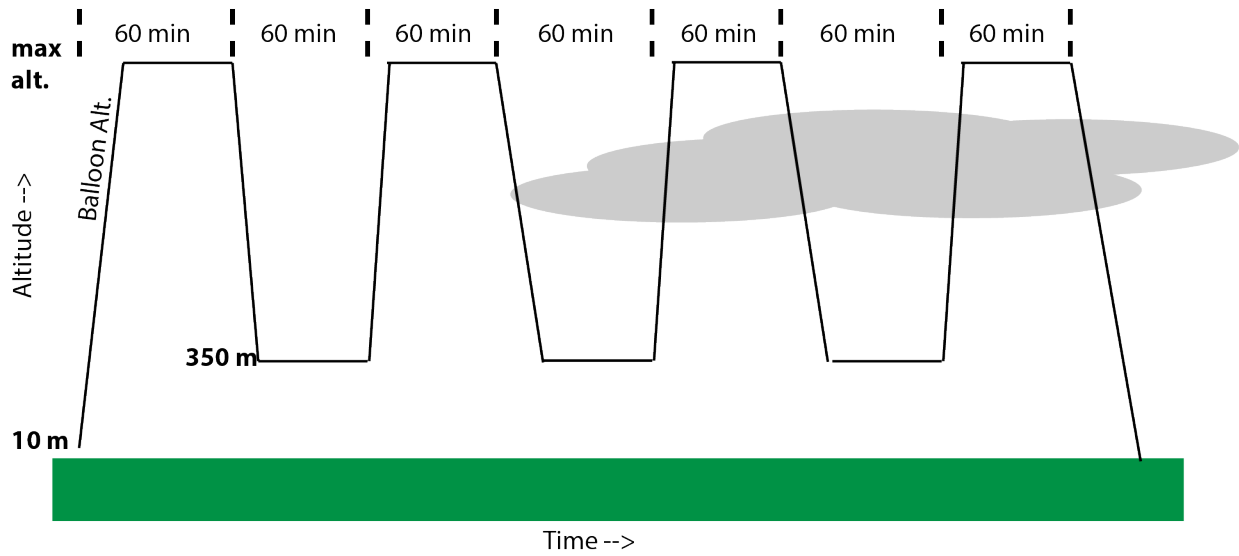
597
598 **Figure 2:** An illustration of the proposed TBS flight pattern for clear or cloudy conditions. The
599 black lines are the proposed flight pattern, with time on the horizontal axis.
600
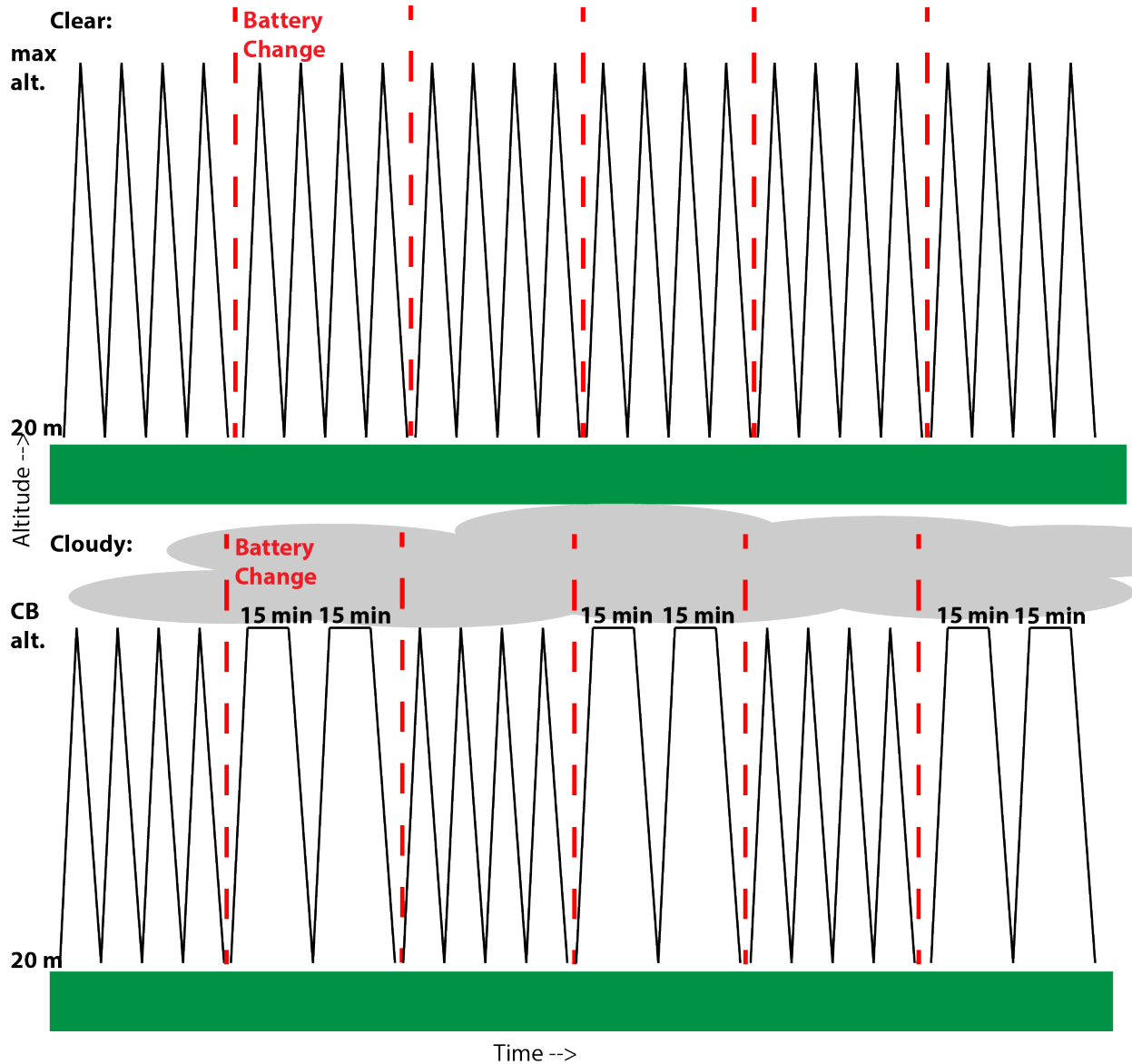
601
602 **Figure 3:** An illustration of the proposed DataHawk2 flight pattern for clear (top) and cloudy
603 (bottom) conditions. The black lines are the proposed flight pattern on a time axis, while the red
604 lines indicate battery changes in between flights.
605
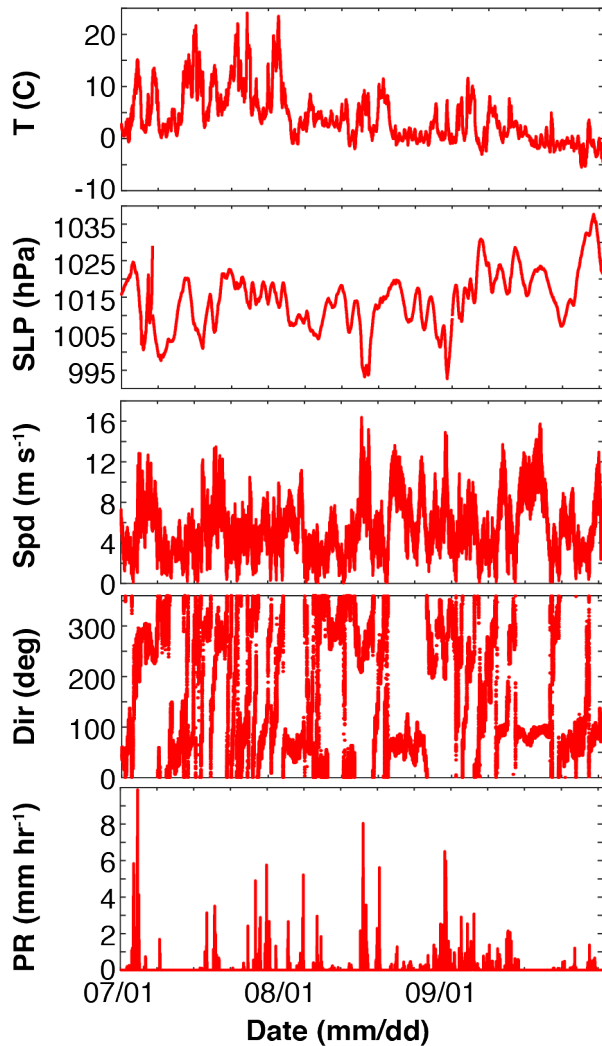
Figure 4: Surface meteorological conditions (1-minute resolution), as measured by instrumentation associated with the Oliktok Point AMF3 during POPEYE. From top to bottom are: 2-meter air temperature, sea level pressure, 10-meter wind speed, 10-meter wind direction and surface precipitation rate.
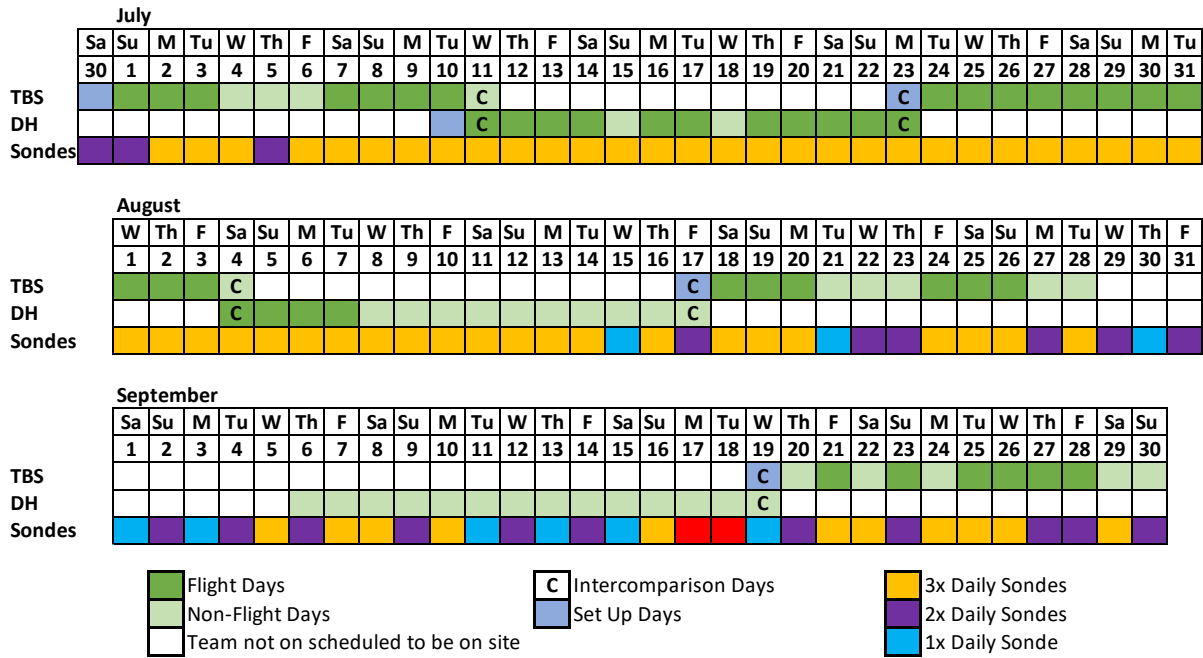
Figure 5: A graphical representation of actual UAS, TBS and radiosonde operations during POPEYE.
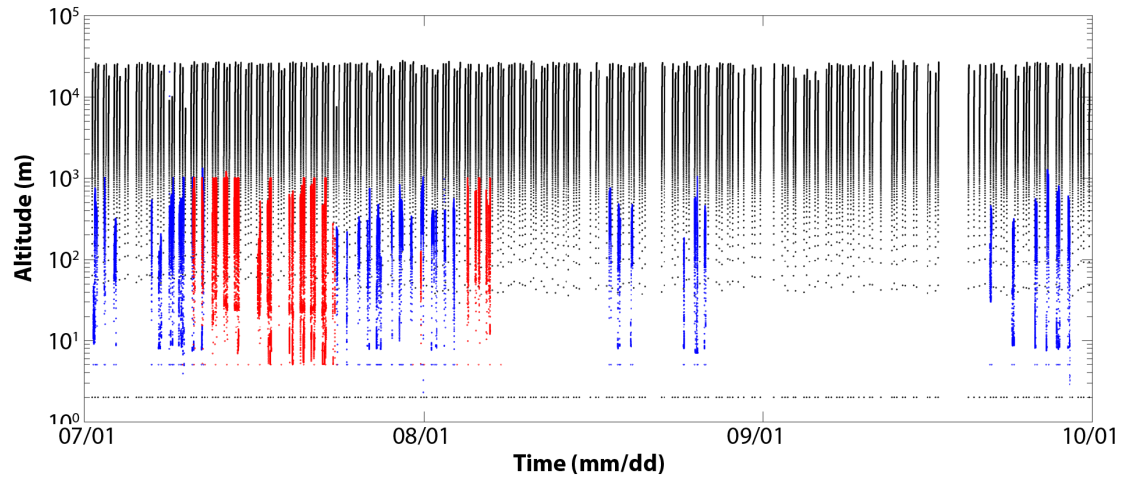
616
617 **Figure 6:** A time-height cross-section illustrating all of the POPEYE radiosonde launches (black
618 dots), DataHawk2 flights (red dots) and tethered balloon flights (blue dots).
619
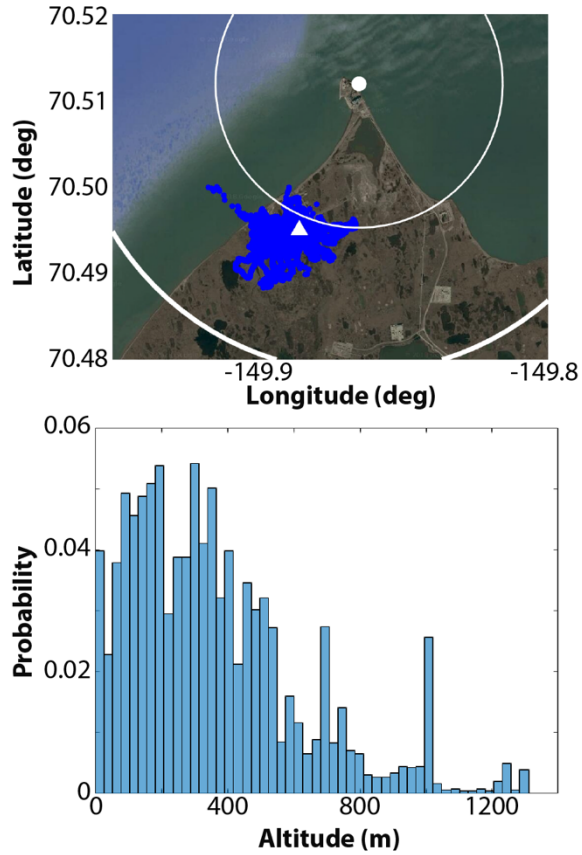
620
621 **Figure 7:** A spatial map of the POPEYE tethered balloon flight locations (top, blue dots), including
622 white range rings at one and two nautical miles demonstrating the extent of R-2204 and the
623 location of the AMF-3 (white triangle). The bottom panel is a relative frequency distribution of
624 the altitudes sampled by the TBS during POPEYE.
625
626
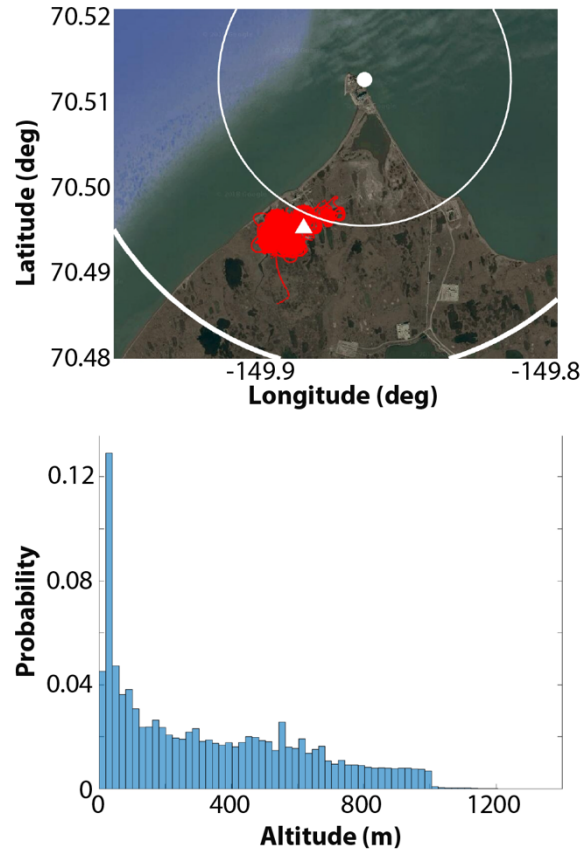
627
628 **Figure 8:** A spatial map of the POPEYE DataHawk2 flight locations (top, red dots), including white
629 range rings at one and two nautical miles demonstrating the extent of R-2204 and the location
630 of the AMF-3 (white triangle). The bottom panel is a relative frequency distribution of the
631 altitudes sampled by the DataHawks during POPEYE.
632

633
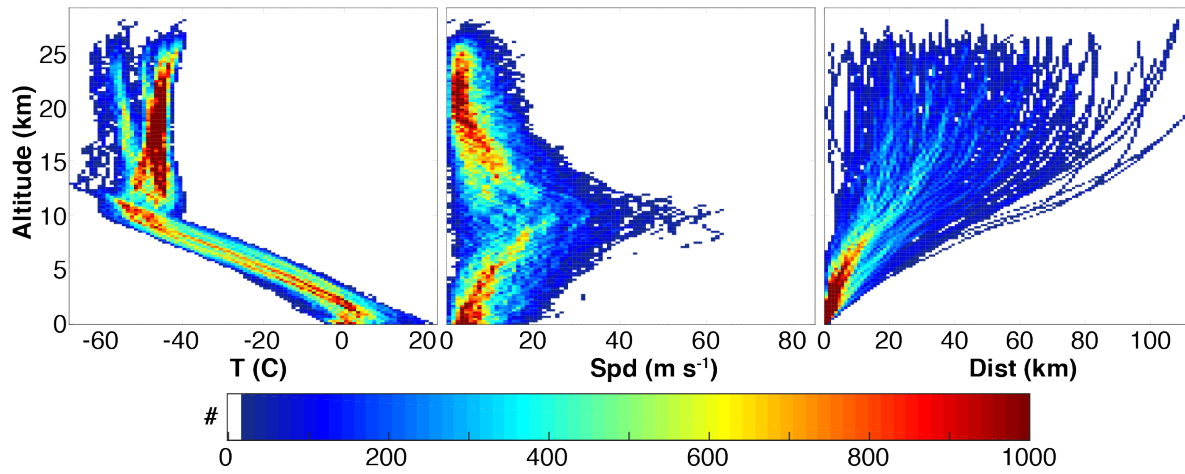
634
635 **Figure 9:** Two-dimensional histograms of radiosonde temperature (left), wind speed (middle),
636 and distance from Oliktok Point (right), with altitude during POPEYE.
637
638
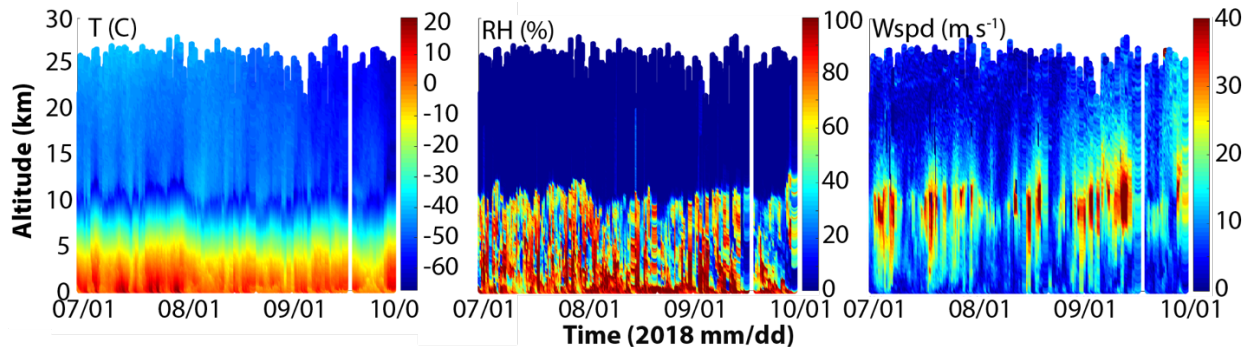
639
640 **Figure 10:** POPEYE radiosonde data, including time-height cross sections of (left to right)
641 temperature, relative humidity and wind speed as observed during the second YOPP Special
642 Observing Period.
643
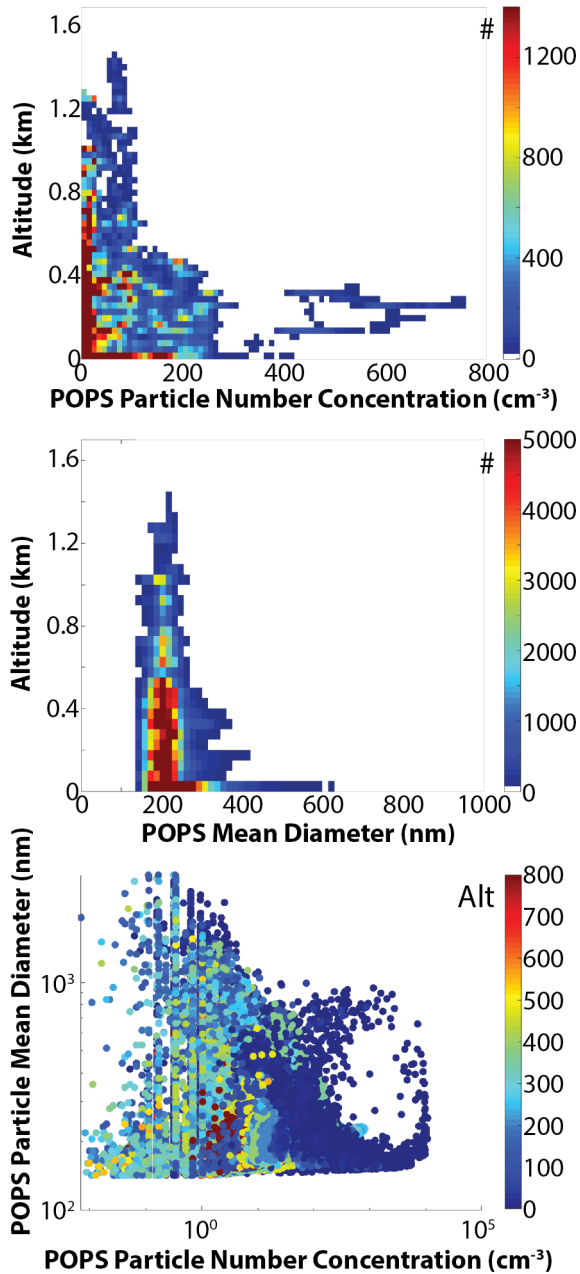
Figure 11: POPEYE aerosol statistics from the POPS sensor. Included are (top to bottom): a two-dimensional histogram of particle number concentrations sampled as a function of height; a two-dimensional histogram of the particle sized detected as a function of height; and a scatter plot showing the relationship between size and number, with colors representing altitude.